Photochemical & Photobiological Sciences

An international journal

www.rsc.org/pps

Volume 8 | Number 1 | January 2009 | Pages 1–124

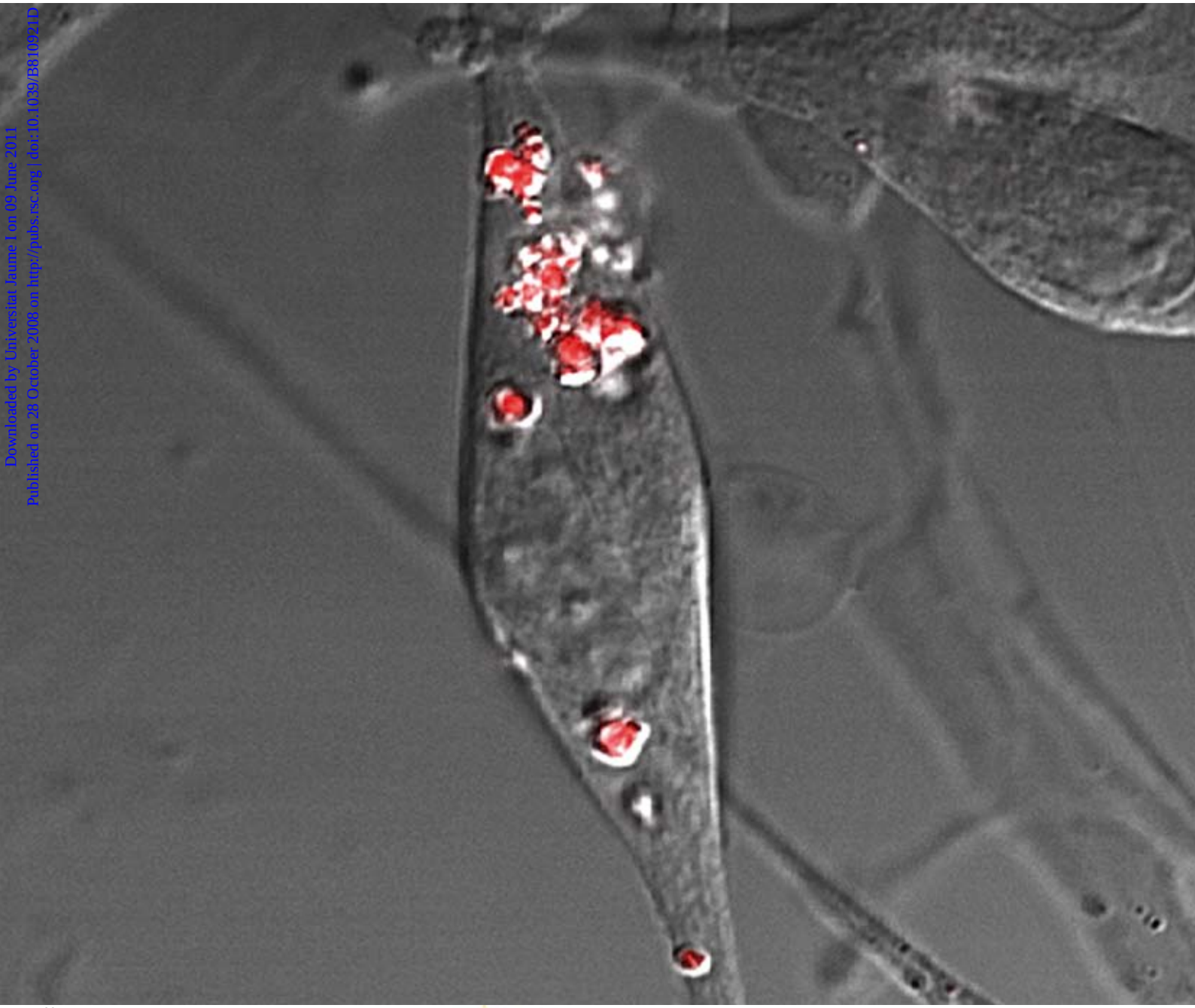

ISSN 1474-905X

RSC Publishing

1474-905X(2009)8:1;1-V

Singlet oxygen generation using a porous monolithic polymer supported photosensitizer: potential application to the photodynamic destruction of melanoma cells†

M. Isabel Burguete,[a] Francisco Galindo,*[a] Raquel Gavara,[a] Santiago V. Luis,*[a] Miguel Moreno,[b] Paul Thomas[c] and David A. Russell*[b]

Received 27th June 2008, Accepted 9th October 2008
First published as an Advance Article on the web 28th October 2008
DOI: 10.1039/b810921d

Photogeneration of singlet oxygen ($^1O_2$) by rose bengal is improved through the use of a porous monolithic polymer (PMP) as a support, as compared to a classic gel-type resin matrix. This type of monolithic polymeric matrix can be made at a multigram scale in quantitative yields enabling the preparation of large amounts of supported photosensitizer at low cost. The singlet oxygen induced oxidation of 9,10-diphenylanthracene has been used as a benchmark reaction, and a comparative study using rose bengal in solution, entrapped within gel-type derived polymer and entrapped within a porous monolithic polymer (PMP) has been performed. The enhanced photoreactivity of the PMP-rose bengal conjugates has been utilised for the successful photodynamic therapy (PDT) of melanoma cells.

Introduction

Oxidations are of broad interest, especially when performed using molecular oxygen ($^3O_2$) as a reactant. However the reactivity of $^3O_2$ is limited, and a large research effort has been focused on the development of new oxidation methods.[1] In this context, singlet oxygen ($^1O_2$), which can be obtained from $^3O_2$, has been shown to be useful in diverse areas such as synthetic chemistry[2] and biomedical sciences.[3] The photochemical generation of singlet oxygen from $^3O_2$ using a suitable photosensitizer can be achieved both in solution and in heterogeneous media. In the heterogeneous case, the pioneering work of Schaap and Neckers[4] with rose bengal[5] immobilized onto low crosslinked polystyrene beads (Merrifield resin) has shown the utility of the approach. In addition to polystyrene beads and rose bengal, other solid supports and photosensitizers have been used to generate singlet oxygen. Thus, recent representative examples of organic and inorganic matrices are polyacrylamine resins,[6] polycyanoacrylates,[7] silica[8] and gold[9] nanoparticles, magnetic carriers,[10]and quantum dots.[11] Even C_{60} fullerene has been incorporated into zeolites[12] in order to create a solid source of $^1O_2$. Many other supports and photosensitizers have been used which have been reported in recent reviews.[13,14] Specifically, the immobilization of rose bengal is covered in detail in the review by De Vos *et al.*[14]

Some of the materials that have been used as supports for photosensitizers require complex and expensive synthetic routes or the reactions are unable to generate multigram quantities of the supported photosensitizer. One type of support, to the best of our knowledge not employed for the immobilization of singlet oxygen photosensitizers, are the so called "porous monolithic polymers" (PMP).[15–17] Such polymers are obtained by unstirred mass polymerisation in the presence of a porogen. The resulting materials consist of a continuous polymer-phase with a high inner porosity. Various applications of these materials for the development of polymer-supported catalytic processes have been reported, in particular taking advantage of their excellent properties for flow processes.[18]

Here we show how immobilization of rose bengal on microparticles derived from a PMP can provide additional benefits for the generation of singlet oxygen, as compared to the rose bengal in solution and to rose bengal supported on the widely employed Merrifield-type resin (gel-type). The resultant photoactive materials, produced at a multigram scale and in a quantitative fashion, are shown here to be active for the generation of $^1O_2$ as exemplified by two paradigmatic applications, one from the synthetic realm and another one from the biomedical field. Firstly, the microparticles have been found to induce effectively the photooxidation of 9,10-diphenylanthracene (DPA) to its endoperoxide. Secondly, the porous monolithic polymer supported photosensitizer has been used to induce the photodynamic destruction of melanoma cancer cells.

Experimental

Materials and methods

p-Chloromethylstyrene (Aldrich, 90%), divinylbenzene (DVB, Fluka, ~80% mixture of isomers; the residual is composed mainly of 1,3- and 1,4-ethylstyrene isomers), 2,2′-azobis(isobutyronitrile) (AIBN, Fluka, ≥98.0%), rose bengal sodium salt (Fluka), tetrabutylammonium hydroxide solution ~25% in MeOH (~0.8 M) (TBAOH solution, Fluka), 9,10-diphenylanthracene (DPA,

[a]*Departamento de Química Inorgánica y Orgánica/UAMOA; Universitat Jaume I/CSIC; Av. Sos Baynat, s/n, 12071, Castellón, Spain. E-mial: francisco.galindo@uji.es, luiss@uji.es*
[b]*School of Chemical Sciences and Pharmacy, University of East Anglia, Norwich, Norfolk, UK NR4 7TJ. E-mail: D.Russell@uea.ac.uk*
[c]*School of Biological Sciences, University of East Anglia, Norwich, Norfolk, UK NR4 7TJ*

† Electronic supplementary information (ESI) available: Fig S1–S6. See DOI: 10.1039/b810921d

Fluka, ≥98.0%), 1-dodecanol (Aldrich, 98%), tetrahydrofuran (Scharlau, synthesis grade), ethyl acetate (Scharlau, synthesis grade), ethanol (Scharlau, 96%), methanol (Scharlau, synthesis grade), methanol (Scharlau, spectroscopy grade), 1,4-dioxane (Scharlau, spectroscopy grade) were used as received. Toluene (Scharlau, synthesis grade) was dried over 4 Å molecular sieves. *N*,*N*′-dimethylformamide was treated previously with anhydrous $MgSO_4$.

To characterize the polymeric materials and to perform the photochemical assays the following techniques were used: Fourier-transform infrared spectroscopy (FT-IR) spectra were recorded using a Perkin Elmer System 2000 FT-IR spectrometer. FT-Raman spectra were recorded using a Perkin Elmer Spectrum 2000 NIR FT-Raman spectrometer. Diffuse reflectance UV-vis absorption spectra were recorded using a Perkin Elmer Lambda 19 spectrophotometer. UV-vis absorption spectra were recorded using a Hewlett-Packard 8453 spectrophotometer. Steady-state fluorescence spectra were acquired using a Spex Fluorolog 3-11 equipped with a 450 W Xenon lamp. Scanning electron micrographs were taken on a LEO 440I microscope equipped with a digital camera. The samples were placed on top of a tin plate and sputtered with Au/Pd in a Polaron SC7610 Sputter Coater from Fisons Instruments. The particle size distribution of the synthesized polymer was determined by means a MASTERSIZER 2000 (MALVERN) laser diffraction instrument. To perform the measurements the sample was suspended in MeOH. The data were analyzed with the software supplied with the instrument.

Synthesis of a porous monolith-type polymer containing rose bengal (P_m-RB). The styrene-based monolith polymer (P_m) was prepared in a similar fashion to those described in the literature,[15] by thermal free radical-initiated polymerization of the monomers in the presence of a porogenic mixture using a glass tube as the mould (1 cm diameter). AIBN (80 mg, 1 wt% with respect to monomers) was dissolved in *p*-chloromethylstyrene (90%, 1.84 g) and divinylbenzene (80% grade, 6.16 g). Then, the porogenic mixture, consisting of 1-dodecanol (10 g) and toluene (2 g) was added. The homogenised polymerization mixture was transferred to several glass tubes and purged with nitrogen in order to remove the dissolved oxygen. Then, the tubes were sealed with rubber septums and placed in a vertical position in a silicon bath heated at 80 °C. The polymerization was allowed to proceed at this temperature for 24 h. The glass tubes were carefully crushed and the polymer was then disaggregated mechanically and washed with tetrahydrofuran for 24 h in a Soxhlet apparatus, in order to remove the porogenic mixture and any other soluble compounds remaining within the polymer. Finally, the polymer was dried in a vacuum oven to obtain P_m in almost a quantitative yield. M = 7.71 g (*ca.* 1.3 mmol Cl g^{-1}). FTIR (KBr) 3020, 2925, 1603, 1266 ($-CH_2Cl$), 710 cm^{-1}; FT-Raman 3055, 2908, 1631, 1611, 1266 ($-CH_2Cl$), 1001, 681 ($-CH_2Cl$), 641.

The polymer P_m (5.77 g, 7.5 mmol of $-CH_2Cl$) and rose bengal sodium salt (8.81 g, 8.66 mmol) were mixed in a 500 ml round-bottom flask and stirred in 400 ml of DMF (treated previously with anhydrous $MgSO_4$) at 80 °C for 8 h in a nitrogen atmosphere. Then, the reaction mixture was cooled to ambient temperature and filtered through a sintered-glass funnel. The obtained resin, P_m-RB, was washed with 250 ml portions of the following solvents: DMF, ethyl acetate, ethanol, ethanol:water 1:1, water, methanol:water 1:1 and methanol. Next, the polymer was extracted with methanol in a Soxhlet apparatus until no visible colour appeared in the solvent. Finally, the light pink polymeric particles were dried in a vacuum oven. M = 5.50 g. FTIR (KBr) 3020, 2925, 1603, 1266, 710 cm^{-1}; FT-Raman 3055, 2909, 1631, 1611, 1512 (RB grafting, low intensity) 1266, 1000, 641 cm^{-1}; RB loading (hydrolysis reaction) = 2 μmol RB g^{-1} of resin; UV-vis diffuse reflectance: λ_{max} = 572 nm; Fluorescence emission: λ_{max} = 593 nm (550 nm exc.).

Synthesis of a gel-type polymer containing RB (P_g-RB). The synthesis of P_g-RB was accomplished following the procedure of Schaap *et al.*[4a] In summary, a Merrifield's peptide resin (15.00 g, 1% cross-linked, 15 mmol of $-CH_2Cl$) and rose bengal sodium salt (15.26 g, 15 mmol) were mixed in a 500 ml round-bottom flask and stirred in 200 ml of DMF (treated previously with anhydrous $MgSO_4$) at 80 °C for 8 h under a nitrogen atmosphere. Then, the reaction mixture was cooled to ambient temperature and filtered through a sintered-glass funnel. The resin was washed with 250-ml portions of the solvents: DMF, ethyl acetate, ethanol, ethanol:water 1:1, water, methanol:water 1:1 and methanol. Next, the polymer beads were extracted with methanol in a Soxhlet apparatus until no visible colour appeared in the solvent. Finally, the dark red beads were dried in a vacuum oven. M = 16.98 g. FTIR (KBr) 3025, 2920, 1736, 1601, 1547, 1344, 1237, 953, 698 cm^{-1}; FT-Raman 3057, 2912, 1614, 1553 (RB grafting), 1498, 1343, 1293, 1235, 1033, 1002, 954 cm^{-1}; RB loading (hydrolysis reaction) = 0.16 mmol RB g^{-1} of resin.

Analytical procedure to estimate the loading of rose bengal in P_m-RB and P_g-RB. The polymeric photosensitizer (20 mg), and tetrabutylammonium hydroxide solution ~0.8 M in MeOH (3 ml) were mixed in a 25 ml round-bottom flask containing 10 ml of 1,4-dioxane. The flask was sealed and the mixture was stirred for 24 h at room temperature. The reaction mixture was then filtered through a sintered-glass funnel and the resin was washed with MeOH until no visible colour appeared in the solvent. The filtrate was transferred into a 100 ml volumetric flask and diluted to 100 ml with MeOH. The final solvent ratio of the solution was MeOH:1,4-dioxane:TBAOH solution, 87:10:3. From the UV-visible absorption spectrum of the solution the amount of free Rose Bengal was determined, using $\varepsilon = 78028 \pm 1291$ l mol^{-1} cm^{-1} at 556 nm from a previous calibration of rose bengal in MeOH:1,4-dioxane:TBAOH (87:10:3).

Photochemical experiments

Photooxidation of DPA with rose bengal sodium salt. The rate of photooxidation of **DPA** (4×10^{-5} M) by singlet oxygen in MeOH was determined for the following concentrations of the photosensitizer: 1.67×10^{-6} M, 6.64×10^{-6} M, 1.44×10^{-5} M, 2.93×10^{-5} M, 5.86×10^{-5} M. In a typical experiment, 3 ml of a solution 4×10^{-5} M of **DPA** in MeOH were transferred into a quartz glass cuvette and an aliquot of a solution 1 mM of rose bengal in MeOH was added to reach the required concentration of the photosensitizer. The air-equilibrated solution was irradiated at room temperature with a Xe lamp (450 W) using a monochromator to select the 556 ± 7 nm window, thus avoiding direct excitation of **DPA**. Stirring was continued throughout the irradiation. The

decreasing absorbance of **DPA** was monitored by means of UV-vis spectroscopy at 391 nm.

Photooxidation of DPA with photosensitizer P_m-RB. The rate of photooxidation of **DPA** (4×10^{-5} M) in MeOH was determined for the following amounts of **P_m-RB** (in parenthesis indicates the equivalent concentration of RB estimated from the loading of the resin): 0.67 mg ml^{-1} (1.34 μM), 1.33 mg ml^{-1} (2.66 μM), 2.67 mg ml^{-1} (5.34 μM), 4.00 mg ml^{-1} (8.00 μM), 6.65 mg ml^{-1} (13.3 μM), 13.30 mg ml^{-1} (26.6 μM). In a typical experiment, 3 ml of a solution 4×10^{-5} M of **DPA** in MeOH were transferred into a quartz glass cuvette containing the corresponding amount of **P_m-RB**. The air-equilibrated solution was irradiated at room temperature with a Xe lamp (450 W) using a monochromator to select the 556 ± 7 nm window. Stirring was continued throughout the irradiation. The decreasing absorbance of **DPA** was monitored by means of UV-visible spectroscopy at 391 nm. Before every measurement the reaction mixture was filtered (syringe filter with 0.2 μm Nylon) to another cuvette in order to remove the polymeric particles in suspension. Additionally, two control experiments (no irradiation) were performed with 1.33 (2.66 μM) and 4.00 mg ml^{-1} (8.00 μM) of the photosensitizer showing no decrease in the **DPA** absorption band. These experiments also assured that no **DPA** were lost during all of the analytical protocols (for instance during the filtration step).

Photooxidation of DPA with photosensitizer P_g-RB. The rate of photooxidation of **DPA** (4×10^{-5} M) in MeOH was determined for the following concentrations of the photosensitizer (in parenthesis indicates the equivalent concentration of rose bengal estimated from the loading of the resin): 4.33 mg ml^{-1} (0.69 mM), 8.33 mg ml^{-1} (1.33 mM), 16.67 mg ml^{-1} (2.67 mM), 33.33 mg ml^{-1} (5.33 mM). In a typical experiment, 3 ml of a solution 4×10^{-5} M of **DPA** in MeOH was transferred into a quartz glass cuvette containing the corresponding amount of **P_g-RB**. The air-equilibrated solution was irradiated at room temperature with a Xe lamp (450 W) using a monochromator to select the 556 ± 7 nm window. Stirring was continued throughout the irradiation. The decreasing concentration of **DPA** was monitored by means of UV-visible spectroscopy at 371 nm. Before each measurement the polymeric beads were allowed to settle to the bottom of the cuvette.

Biological evaluation

Culture and imaging of the melanoma cells. Melanoma (B16/F10) cells (European Collection of Animal Cell Cultures, Porton Down, UK) were routinely cultured in 75 cm^3 tissue culture flasks using the following culture medium: Dulbecco's Modified Eagle Medium (DMEM) supplemented with 10% fetal calf serum (FCS) and 1% penicillin-streptomycin (P-S) (Invitrogen Life Sciences, Paisley, UK). Leibowitz L-15 medium (Sigma) was used to rinse the cells before imaging. Imaging medium 120 mM NaCl, 5 mM KCl, 2 mM $CaCl_2$, 1 mM $MgCl_2$, 1 mM NaH_2PO_4, 1 mM $NaHCO_3$, 11 mM glucose, 2 mM glutamine, 2% (v/v) Basal Medium Eagle (BME) amino acids solution, 1 mg ml^{-1} Bovine Serum Albumin (BSA). A 25 mM HEPES/NaOH buffer, pH 7.2 (Sigma), was used for culturing the cells during imaging. To assess polymer uptake by the melanoma cells and cellular morphology post-PDT, confocal laser scanning microscopy was used. Cells (25×10^4 cells) were cultured on 42 mm round coverslips in a Petri dish with 5 ml of the culture medium for 48 h. Cells were then incubated with 10 ng ml^{-1} final concentration of the **P_m-RB** polymer beads for approximately 16 h. For imaging, the cells were placed in a chamber and rinsed three times with 2 ml of rinsing medium, covered with 2 ml of imaging medium and taken to the microscope where the cells were placed on a heated stage at 37 °C. The cells were imaged with a confocal laser scanning microscope (Leica TCS SP2 UV system) using a 543 nm laser (HeNe) set to 10–15% power; simultaneously a differential interference contrast (DIC) image was acquired with the same laser. Fluorescence emission from the rose bengal was collected from 560 to 750 nm. To stimulate the production of singlet oxygen, both 488 nm (Ar^+) and 543 nm (HeNe) lasers at full power were used. After activation with lasers, cells were incubated for 90 min and then imaged. Blank experiments were prepared analogously.

Results and discussion

A porous monolithic polymer containing reactive chloromethyl groups was synthesized by polymerization of a mixture of divinylbenzene and chloromethylstyrene (80:20 molar) in the presence of dodecanol:toluene (5:1, w:w) as the porogens (3:2 w:w, porogens:monomers ratio).[15,18] This procedure led to a continuous rod of several cm length and *ca.* 1 cm width. This material (**P_m**) was then ground to obtain small-sized particles. Reaction of this powdered resin (1.3 mmol Cl g^{-1} polymer) with rose bengal (disodium salt)[4] in DMF at 80 °C for 8 h lead to the resin **P_m-RB** displaying a pink colour that was indicative of the anchoring of rose bengal to the polymer (see Scheme 1). It is worth noting that the **P_m** bound rose bengal was obtained in a multigram scale (5–6 g) in a four-step process, which represents an important advantage over other time-consuming methodologies that may lead to sophisticated matrices but which may be only available at the milligram, or lower, scale. Additionally, while many types of $^1O_2$ generators have been developed to date, the well-known rose bengal is still used for the generation of $^1O_2$ when anchored to solid supports,[19] and hence we selected this dye as an appropriate photosensitizer for this study. However, the method presented

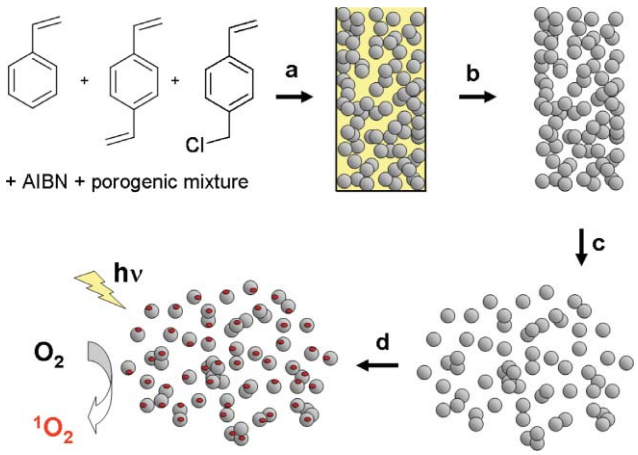

Scheme 1 (a) Polymerisation of the vinyl monomers. (b) Unmoulding and extraction of the porogenic mixture. (c) Dissaggregation of the porous monolithic polymer rod. (d) Derivatization with rose bengal.

herein should be compatible with any other photosensitizers of interest, if stable at the grafting conditions.

Steady-state fluorescence and diffuse-reflectance UV-vis spectroscopies were used to confirm the presence of rose bengal attached to $\mathbf{P_m}$ which can be seen from the typical spectral signature of rose bengal (see ESI,† Figure S1). The recorded fluorescence and absorption maxima are located at: $\lambda_{em} = 593$ nm, $\lambda_{exc} = 572$ nm, $\lambda_{dr\text{-}uv} = 572$ nm respectively.

The basic hydrolysis of rose bengal from the polymeric support and the UV-vis measurement of the hydrolisate enabled determination of the content of the photosensitizer to be 2 μmol g^{-1} on the **P_m-RB**. Low efficiencies for the grafting procedure have been reported in such monolithic polymers and hence the low loading in **P_m-RB** could be due to the extensive crosslinking of this macroporous material.[15,17]

Optical and scanning electron microscopy (SEM, see ESI,† Figure S2 and S3 respectively) revealed that **P_m-RB** consisted of clusters of small microglobules, with each globule ca. 1 μm in diameter. The analysis of **P_m-RB** by wet laser diffraction afforded a size distribution with a maximum peak at 12.4 μm (see ESI,† Figure S4). The polymeric photosensitizer appears to be composed of three populations of large (ca. 12 μm), medium (ca. 3 μm) and small (ca. 0.5 μm) particles.

In order to demonstrate the ability of the **P_m-RB** photosensitizer to generate $^1O_2$, the new material was used as a photocatalyst for the chemical oxidation of a well-known $^1O_2$ acceptor, and as a photodynamic agent for the induction of cell death in a culture of melanoma cells. The oxidation of 9,10-diphenylanthracene (**DPA**) with $^1O_2$ yields a transannular endoperoxide as shown in Scheme 2. This acceptor was chosen because of its high reaction rate constant[20] with $^1O_2$ and the fact that it does not absorb at the wavelength used for irradiation of the samples (556 ± 7 nm). Kinetic experiments were performed by monitoring the bleaching of the absorption band of **DPA** in methanol (350–400 nm) as a function of the irradiation time and at several concentrations of **P_m-RB** (Fig. 1). Rose bengal in solution, as its disodium salt, was used as a control.

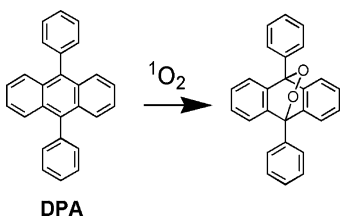

Scheme 2 Singlet oxygen oxidation of **DPA** to its endoperoxide.

Irradiation of all the samples was achieved by passing the light of a Xe lamp through a monochromator in order to select the 556 ± 7 nm window, as described in the experimental section. The resulting kinetic profiles were linear with time for both rose bengal and **P_m-RB** (Fig. 2 and 3 respectively). As shown in Fig. 4, the oxidation of **DPA** sensitized by increasing amounts of rose bengal in solution, attained a limiting observed constant of $k_{obs} \sim 7.5 \times 10^{-3}$ min^{-1}. However, when the oxidation of **DPA** was sensitized by the functional macroporous resin **P_m-RB**, the maximum k_{obs} measured was 3.7×10^{-2} min^{-1}. In order to eliminate the possibility that physical adsorption of **DPA** onto the polymer surface was the cause of the reduction of **DPA** from the solution,

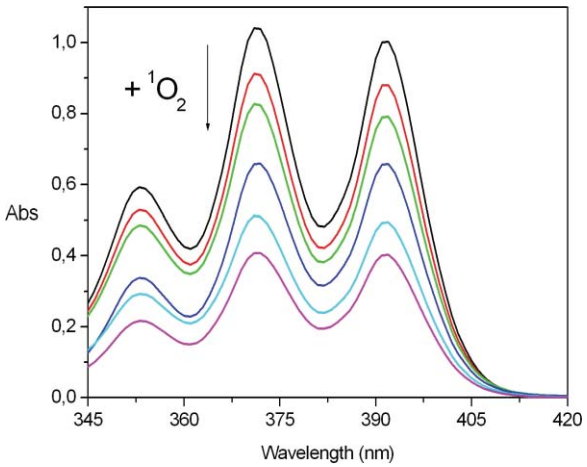

Fig. 1 Representative kinetic experiment. Bleaching of the absorption bands of **DPA** (4×10^{-5} M initially, in MeOH) when irradiated using **P_m-RB** (6.65 mg ml^{-1}) as a photosensitizer. The spectra correspond to the following irradiation times (from top to bottom): 0, 5, 10, 15, 20 and 25 min.

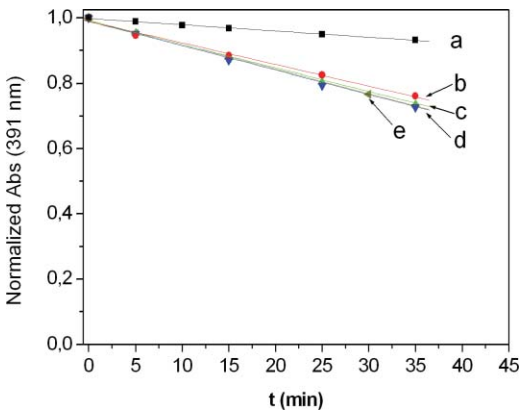

Fig. 2 Irradiation of **DPA** (4×10^{-5}M, MeOH) in the presence of rose bengal in solution at several concentrations of sensitizer. (a) 1.67×10^{-6} M; (b) 6.64×10^{-6} M; (c) 1.44×10^{-5} M; (d) 2.93×10^{-5} M; (e) 5.86×10^{-5} M.

the corresponding dark experiments using **P_m-RB** were conducted, with no change in the **DPA** absorption band observed (Fig. 3a and b). Additionally, it should be noted that no rose bengal was detected in the solution after irradiation of **P_m-RB**, which removes the possibility that sensitisation was induced by the leaching of the rose bengal photosensitizer from the matrix.

An increase in the $^1O_2$ quantum yield generation by **P_m-RB** relative to rose bengal in solution is not expected since rose bengal in methanol is known to possess a rather high efficiency for the generation of this reactive species ($\phi_\Delta = 0.76$).[5] Thus the differences in k_{obs} cannot be directly translated into differences in ϕ_Δ, since the obtained value for **P_m-RB** would be higher than unity. The heterogeneous nature of **P_m-RB** together with its morphology could account for the apparent increased efficiency of oxidation. Most likely, light scattering by the microparticles plays a significant role which may explain the results. On the other hand a higher local concentration of reactive species at the surface of the polymeric sensitizer (reversible and transient surfacial adsorption of DPA onto the microspheres, or longer lifetime of $^1O_2$ close to the hydrophobic polymer matrix), could have also some effect.

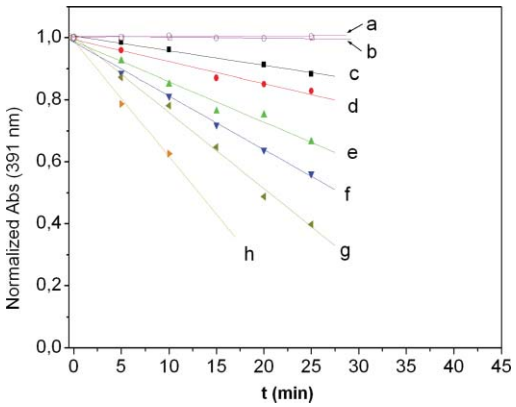

Fig. 3 Irradiation of **DPA** (4×10^{-5} M, MeOH) in the presence of **P_m-RB** at several concentrations, including two dark controls (a) and (b). (a) 1.33 mg ml^{-1} (2.66×10^{-6} M equiv. RB); (b) 4.00 mg ml^{-1} (8.00×10^{-6} M equiv. RB); (c) 0.67 mg ml^{-1} (1.34×10^{-6} M equiv. RB); (d) 1.33 mg ml^{-1} (2.66×10^{-6} M equiv. RB); (e) 2.67 mg ml^{-1} (5.34×10^{-6} M equiv. RB); (f) 4.00 mg ml^{-1} (8.00×10^{-6} M equiv. RB); (g) 6.65 mg ml^{-1} (1.33×10^{-5} M equiv. RB); (h) 13.30 mg ml^{-1} (2.66×10^{-5} M equiv. RB).

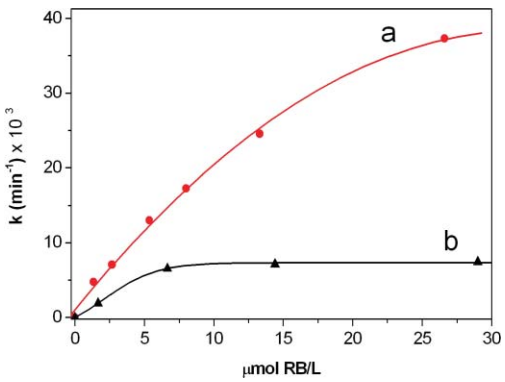

Fig. 4 Kinetics of the photooxidation of **DPA** in methanol. k_{obs} *vs.* concentration of rose bengal (which was estimated in the case of supported RB, according to the loading of rose bengal of **P-RB** and to the added amount of resin in each experiment.) (a) **P_m-RB**; (b) rose bengal in solution.

A rose bengal coated gel-type resin (**P_g-RB**) was also prepared, characterized and used for the oxidation of **DPA**. The beads of this kind of polymer have a significantly greater size (in our case 40–70 µm diameter) than the **P_m-RB** (12.4 µm diameter) and also a lower permanent specific surface, and hence it would not be expected to produce the enhanced singlet oxygen production through the effects of light scattering and/or transient surfacial adsorption. The maximum observed rate for the oxidation of **DPA** promoted by **P_g-RB** was of 6×10^{-3} min^{-1} (see ESI,† Figure S5). In order to illustrate the size of the gel-type resin, a SEM micrograph of **P_g-RB** is shown in Figure S3,† which can be compared to Figure S2.† In Table 1 the kinetic constants measured for the rose bengal in solution and both the gel-type polymer and the porous monolithic polymer supports are shown.

Since singlet oxygen is important for biomedical applications, the utility of the newly developed polymeric material was tested for the destruction of cancerous cells. Photodynamic therapy (PDT)[3] of cancer involves the uptake of non-toxic photosensitizers in tumour tissues and subsequent activation by light to generate cytotoxic $^1O_2$. Particles of **P_m-RB** were incubated with a culture of

Table 1 Kinetic constants measured in this study

Photosensitizer	Conc. Polymer/mg ml^{-1}	Conc. RB/M[a]	$k/10^{-3}$ min^{-1}
RB	—	1.67×10^{-6}	1.9
	—	6.64×10^{-6}	6.6
	—	1.44×10^{-5}	7.2
	—	2.93×10^{-5}	7.5
	—	5.86×10^{-5}	7.4
P_m-RB	0.67	1.34×10^{-6}	4.8
	1.33	2.66×10^{-6}	7.1
	2.67	5.34×10^{-6}	13.0
	4.00	8.00×10^{-6}	17.3
	6.65	1.33×10^{-5}	24.6
	13.30	2.66×10^{-5}	37.3
P_g-RB	4.33	6.90×10^{-4}	2.9
	8.33	1.33×10^{-3}	4.2
	16.67	2.67×10^{-3}	6.3
	33.33	5.33×10^{-3}	5.8

[a] Calculated in the case of supported RB according to the loading of RB and to the added amount of resin in each experiment.

melanoma (B16/F10) cells. The uptake of the particles by the cells following 16 h incubation was established by confocal fluorescence microscopy taking advantage of the intrinsic fluorescence of the photosensitizer ($\phi_F = 0.08$ in MeOH).[5] The combined differential interference contrast (DIC) and fluorescence microscopy images show the presence of the **P_m-RB** particles distributed within, or perhaps on the membrane surface, of the melanoma cells (Fig. 5). From this figure it appears that only the smaller sized particles have entered the cells.

A sample of the **P_m-RB** incubated cells was irradiated in order to test the ability of the microparticles to induce cell-death. Parameters for PDT were fixed based on our previously reported results using phthalocyanine stabilised gold nanoparticles.[9] A final concentration of 10 ng ml^{-1} of **P_m-RB** was incubated for ca. 16 hours and a period of irradiation of the cells of 10 min using the 488 (Ar) and 543 nm (HeNe) lasers at full power. The efficiency of PDT was demonstrated by imaging cells before (Fig. 6A) and after (Fig. 6B) treatment and studying the viability as a function of the cell morphology. Hence, 90 min after PDT, the morphology of the melanoma cells changed dramatically. Cells began to show the presence of blebs (black arrows in Fig. 6B) and vacuoles (white arrows in Fig. 6B) as well as condensation of the nucleus (red arrow in Fig. 6B). These cellular features are not present in 'healthy' melanoma cells before treatment and are indicative of cell mortality induced by photodynamic action.

Kochevar *et al.* have shown that activation of rose bengal by visible light produces predominately singlet oxygen and consequently observed extensive apoptosis in HL-60 cells.[21] A cell undergoing apoptosis shows a characteristic morphology, the cell membrane shows irregular buds (blebs), the cytoplasm appears dense, chromatin undergoes condensation into compact patches and the organelle appear tightly packed.[22] The cellular features, which were all observed (Fig. 6B) under our experimental conditions, suggest that mortality of the melanoma cells was induced by apoptosis, although other mechanisms cannot be disregarded.[23]

Control experiments were performed using **P_m**, the matrix used to synthesize **P_m-RB** but without grafted rose bengal. The parameters used were the same as above and the combined DIC and fluorescence microscopy images (see ESI,† Figure S6) clearly

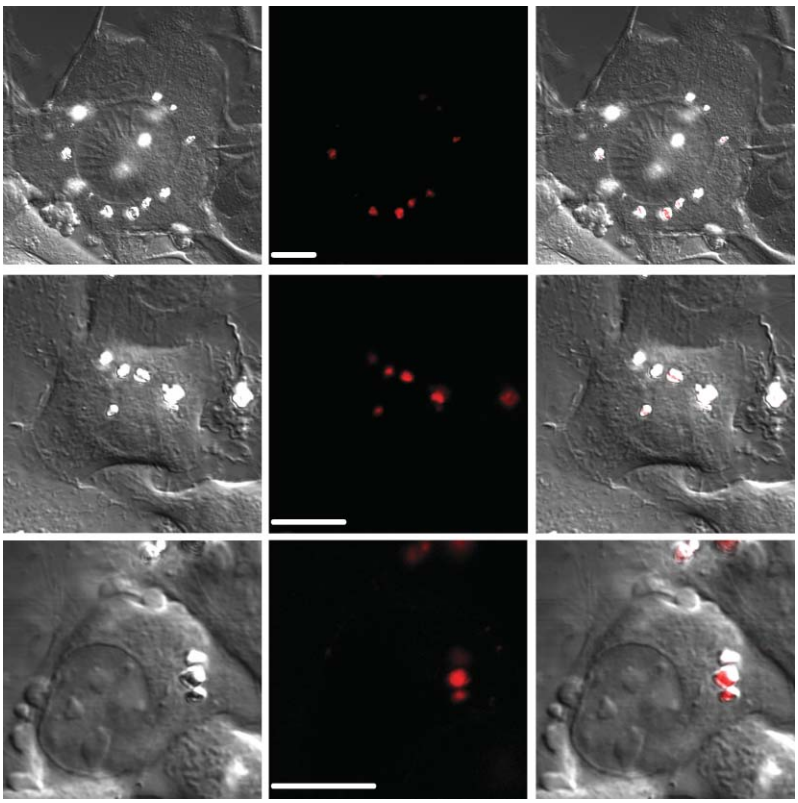

Fig. 5 Confocal laser scanning microscopy images of melanoma cells with microparticles of **P_m-RB**. Left hand side; DIC (differential interference contrast) images. Centre; fluorescence images. Right hand side; the combined DIC and fluorescence images. Scale bars = 10 μm.

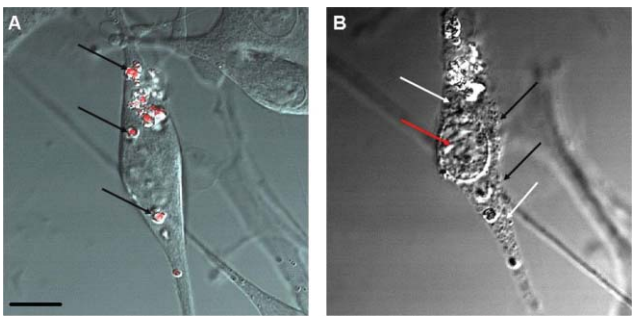

Fig. 6 Combined confocal fluorescence and DIC (differential interference contrast) images of: (A) a pre-irradiation image of **P_m-RB** particles (10 ng ml^{-1}) incubated with melanoma (B16/F10) cells for 16 h and (B) 90 min post-irradiation image of B16/F10 melanoma cells. The cellular morphology in (B) shows the presence of blebs and vacuoles (white arrows), structures which are absent in the pre-PDT treated cells shown in (A). Scale bar = 10 μm.

show the presence of non-fluorescent particles (white arrows) within the cells. Following irradiation the cellular morphology did not change (Figure S6), indicating that the melanoma cell remains viable. Melanoma cells were also subjected to the same irradiation treatment but with no particles at all. Combined DIC and fluorescence microscopy images showed the absence of changes in the cellular morphology following laser irradiation. These two control experiments confirm the induction of photodynamic mortality of the melanoma cells by the porous monolithic polymer bound photosensitizer.[24]

Conclusion

In summary, we have shown that porous monolithic polymers can be used as an insoluble support for photooxidation reactions through the grafting of a prototypical $^1O_2$ generator such as rose bengal. In this way, excellent photocatalytic particles of **P_m-RB** can be prepared. These PMP photosensitizers are able to generate $^1O_2$ efficiently as shown with the oxidation of **DPA** and subsequently, the photodynamic destruction of melanoma cells. The effect of particle size, crosslinking degree, oxygen solubility in the matrix (both $^3O_2$ and $^1O_2$) and adsorption of reactants on the surface of the photosensitizer could contribute to the photocatalytic efficiency. Low cost and multigram scale of photosensitizer production are two advantages of PMPs over other classes of supports for oxidations with $^1O_2$. In comparison with the classical rose bengal-coated gel-type resin, and to rose bengal in solution, the PMP matrix displays a significantly higher oxidation efficiency of **DPA** in methanol. While gel-type rose bengal-loaded resin and rose bengal in solution attained a limiting value for their rate constants of 6×10^{-3} min^{-1} and 7.5×10^{-3} min^{-1}, respectively, for the oxidation of **DPA**, the same process using **P_m-RB** can be carried out with a rate constant of up to 3.7×10^{-2} min^{-1}. The singlet oxygen induced destruction of melanoma cells using the polymer supported rose bengal (**P_m-RB**) has shown the utility of

such porous monolithic polymers as a suitable support for the delivery of photosensitizer agents for photodynamic therapy.

Acknowledgements

Financial support from the Spanish MEC (CTQ2005-08016-003), GVA (projects GV/2007/277, ARVIV/2007/079, ARVIV/2007/081) and F. Caixa Castelló-UJI (project P1·1A2007-05) is acknowledged. D.A.R. acknowledges financial support from Cancer Research UK (Grant number C22031/A7097). F.G. thanks the support from MEC (Ramón y Cajal Program). R.G. thanks the support from MEC (FPI). The technical support from SCIC (UJI) is also acknowledged.

Notes and references

1 L. Alaerts, J. Wahlen, P. A. Jacobs and D. E. De Vos, Recent progress in the immobilization of catalysts for selective oxidation in the liquid phase, *Chem. Commun.*, 2008, 1727–1737.
2 E. L. Clennan and A. Pace, Advances in singlet oxygen chemistry, *Tetrahedron*, 2005, **61**, 6665–6691; M. C. DeRosa and R. J. Crutchley, Photosensitized singlet oxygen and its applications, *Coord. Chem. Rev.*, 2002, **233**, 351–371.
3 *Nanomaterials for Cancer Therapy*, ed. C. S. S. R. Kumar, Wiley-VCH, Weinheim, 2006; A. Juzeniene, Q. Peng and J. Moan, Milestones in the development of photodynamic therapy and fluorescence diagnosis, *Photochem. Photobiol. Sci.*, 2007, **6**, 1234–1245; I. J. Macdonald and T. J. Dougherty, Basic principles of photodynamic therapy, *J. Porph. Phthal.*, 2001, **5**, 105–129.
4 E. C. Bloosey, D. C. Neckers, A. L. Thayer and A. P. Schaap, Polymer-based sensitizers for photooxidations, *J. Am. Chem. Soc.*, 1973, **95**, 5820–5822; A. P. Schaap, A. L. Thayer, E. C. Blossey and D. C. Neckers, Polymer-based sensitizers for photooxidations. II, *J. Am. Chem. Soc.*, 1975, **97**, 3741–3745; J. Paczkowski and D. C. Neckers, Polymer-based sensitizers for the formation of singlet oxygen. New studies of polymeric derivatives of rose bengal, *Macromolecules*, 1985, **18**, 1245–1253; J. Paczkowski and D. C. Neckers, Photochemical properties of rose bengal. 11. Fundamental studies in heterogeneous energy transfer, *Macromolecules*, 1985, **18**, 2412–2418; A. P. Schaap, A. L. Thayer, K. A. Zaklika and P. C. Valenti, Photooxygenations in aqueous solution with a hydrophilic polymer-immobilized photosensitizer, *J. Am. Chem. Soc.*, 1979, **101**, 4016–4017.
5 D. C. Neckers, Rose Bengal, *J. Photochem. Photobiol. A: Chem.*, 1989, **47**, 1–29; C. R. Lambert and I. E. Kochevar, Does rose bengal triplet generate superoxide anion?, *J. Am. Chem. Soc.*, 1996, **118**, 3297–3298.
6 M. J. Moreno, E. Monson, R. G. Reddy, A. Rehemtulla, B. D. Ross, M. Philbert, R. J. Schneider and R. Kopelman, Production of singlet oxygen by $Ru(dpp(SO_3)_2)_3$ incorporated in polyacrylamide PEBBLES, *Sens. Actuators, B*, 2003, **90**, 82–89; W. Tang, H. Xu, R. Kopelman and M. A. Philbert, Photodynamic characterization and in vitro application of methylene blue-containing nanoparticle platforms, *Photochem. Photobiol.*, 2005, **81**, 242–249; D. Gao, H. Xu, M. A. Philbert and R. Kopelman, Ultrafine hydrogel nanoparticles: synthetic approach and therapeutic application in living cells, *Angew. Chem. Int. Ed.*, 2007, **46**, 2224–2227.
7 A. Labib, V. Lenaerts, F. Chouinard, J. C. Leroux, R. Ouellet and J. E. van Lier, Biodegradable nanospheres containing phthalocyanines and naphthalocyanines for targeted photodynamic tumor therapy, *Pharm. Res.*, 1991, **8**, 1027–1031; E. Allemann, J. Rousseau, N. Brasseur, V. S. Kudrevich, K. Lewis and J. E. van Lier, Photodymamic therapy of tumours with hexadecafluoro zinc phthalocyanine formulated in peg-coated poly(lactic acid) nanoparticles, *Int. J. Cancer*, 1996, **66**, 821–824.
8 F. Yan and R. Kopelman, The embedding of meta-tetra(hydroxyphenyl)-chlorin into silica nanoparticle platforms for photodynamic therapy and their singlet oxygen production and pH-dependent optical properties, *Photochem. Photobiol.*, 2003, **78**, 587–591; I. Roy, T. Y. Ohulchanskyy, H. E. Pudavar, E. J. Bergey, A. R. Oseroff, J. Morgan, T. J. Dougherty and P. N. Prasad, Ceramic-based nanoparticles entrapping water-insoluble photosensitizing anticancer drugs: a novel drug-carrier system for photodynamic therapy, *J. Am. Chem. Soc.*, 2003, **125**, 7860–7865; T. Y. Ohulchanskyy, I. Roy, L. N. Goswami, Y. Chen, E. J. Bergey, R. K. Pandey, A. R. Oseroff and P. N. Prasad, Organically modified silica nanoparticles with covalently incorporated photosensitizer for photodynamic therapy of cancer, *Nano Lett.*, 2007, **7**, 2835–2842; S. Kim, T. Y. Ohulchanskyy, H. E. Pudavar, R. K. Pandey and P. N. Prasad, Organically modified silica nanoparticles co-encapsulating photosensitizing drug and aggregation-enhanced two-photon absorbing fluorescent dye aggregates for two-photon photodynamic therapy, *J. Am. Chem. Soc.*, 2007, **129**, 2669–2675.
9 D. C. Hone, P. I. Walker, R. Evans-Gowing, S. FitzGerald, A. Beeby, I. Chambrier, M. J. Cook and D. A. Russell, Generation of cytotoxic singlet oxygen *via* phthalocyanine-stabilized gold nanoparticles: a potential delivery vehicle for photodynamic therapy, *Langmuir*, 2002, **8**, 2985–2987; M. E. Wieder, D. C. Hone, M. J. Cook, M. M. Handsley, J. Gavrilovic and D. A. Russell, Intracellular photodynamic therapy with photosensitizer-nanoparticle conjugates: cancer therapy using a 'Trojan horse', *Photochem. Photobiol. Sci.*, 2006, **5**, 727–734.
10 D. B. Tada, L. L. R. Vono, E. L. Duarte, R. Itri, P. K. Kiyohara, M. S. Baptista and Liane M. Rossi, Methylene blue-containing silica-coated magnetic particles: a potential magnetic carrier for photodynamic therapy, *Langmuir*, 2007, **23**, 8194–8199.
11 L. Shi, B. Hernandez and M. Selke, Singlet oxygen generation from water-soluble quantum dot-organic dye nanocomposites, *J. Am. Chem. Soc.*, 2006, **128**, 6278–6279; A. C. S. Samia, X. Chen and C. Burda, Semiconductor quantum dots for photodynamic therapy, *J. Am. Chem. Soc.*, 2003, **125**, 15736–15737.
12 M. S. Galletero, H. García and J. L. Bourdelande, Dramatic persistence (minutes) of the triplet excited state and efficient singlet oxygen generation for C_{60} incorporated in Y zeolite and MCM-41 silicate, *Chem. Phys. Lett.*, 2003, **370**, 829–833.
13 S. Wang, R. Gao, F. Zhou and M. Selke, Nanomaterials and singlet oxygen photosensitizers: potential applications in photodynamic therapy, *J. Mater. Chem.*, 2004, **14**, 487–493.
14 J. Wahlen, D. E. De Vos, P. A. Jacobs and P. L. Alsters, Solid materials as sources for synthetically useful singlet oxygen, *Adv. Synth. Catal.*, 2004, **346**, 152–164.
15 F. Svec and J. M. J. Fréchet, New designs of macroporous polymers and supports: from separation to biocatalysis, *Science*, 1996, **273**, 205–211; D. C. Sherrignton, Preparation, structure and morphology of polymer supports, *Chem. Commun.*, 1998, 2275–2286; *Synthesis and separations using functional polymers*, ed. D. C. Sherrington and P. Hodge, John Wiley & Sons Ltd, Chichester, 1988; *Polymeric materials in organic synthesis and catalysis*, ed. M. R. Buchmeiser, Wiley-VCH, Weinheim, 2003.
16 A. Chighine, G. Sechi and M. Bradley, Tools for efficient high-throughput synthesis, *Drug Disc. Today*, 2007, **12**, 459–464; A. Solinas and M. Taddei, Solid-supported reagents and catch-and-release techniques in organic synthesis, *Synthesis-Stuttgart*, 2007, 2409–2453; B. M. L. Dioos, I. F. J. Vankelecom and P. A. Jacobs, Aspects of immobilisation of catalysts on polymeric supports, *Adv. Synth. Catal.*, 2006, **348**, 1413–1446; A. Chesney, Selected highlights in the application of ion-exchangers: as supports for reagents in organic synthesis, *Green Chem.*, 1999, **1**, 209–219.
17 F. Svec and J. M. J. Fréchet, Continuous rods of macroporous polymer as high-performance liquid chromatography separation media, *Anal. Chem.*, 1992, **64**, 820–822; C. Vicklund, F. Svec, J. M. J. Fréchet and K. Irgum, Monolithic, "molded", porous materials with high flow characteristics for separations, catalysis, or solid-phase chemistry: control of porous properties during polymerization, *Chem. Mater.*, 1996, **8**, 744–750; E. C. Peters, F. Svec and J. M. J. Fréchet, Rigid Macroporous Polymer Monoliths, *Adv. Mater.*, 1999, **11**, 1169–1181; M. R. Buchmeiser, Polymeric monolithic materials: syntheses, properties, functionalization and applications, *Polymer*, 2007, **48**, 2187–2198.
18 M. I. Burguete, A. Cornejo, E. García-Verdugo, J. García, M. J. Gil, S. V. Luis, V. Martinez-Merino, J. A. Mayoral and M. Sokolova, Bisoxazoline-functionalised enantioselective monolithic mini-flow-reactors: development of efficient processes from batch to flow conditions, *Green Chem.*, 2007, **9**, 1091–1096; M. I. Burguete, A. Cornejo, E. García-Verdugo, M. J. Gil, S. V. Luis, J. A. Mayoral, V. Martinez-Merino and M. Sokolova, Pybox monolithic miniflow reactors for continuous asymmetric cyclopropanation reaction under conventional and supercritical conditions, *J. Org. Chem.*, 2007, **72**, 4344–4350; N. Karbass, V. Sans, E. García-Verdugo, M. I. Burguete and S. V. Luis, Pd(0) supported onto monolithic polymers containing

IL-like moieties. Continuous flow catalysis for the Heck reaction in near-critical EtOH, *Chem. Commun.*, 2006, 3095–3097; G. Jas and A. Kirschning, Continuous flow techniques in organic synthesis, *Chem. Eur. J.*, 2003, **9**, 5708–5723; M. I. Burguete, E. García-Verdugo, M. J. Vicent, S. V. Luis, H. Pennemann, N. Graf, von Keyserling and J. Martens, New Supported β-Amino Alcohols as Efficient Catalysts for the Enantioselective Addition of Diethylzinc to Benzaldehyde under Flow Conditions, *Org. Lett.*, 2002, **4**, 3947–3950; B. Altava, M. I. Burguete, J. M. Fraile, J. I. Garcia, S. V. Luis, J. A. Mayoral and S. V. Luis, How important is the inert matrix of supported enantiomeric catalysts? Reversal of topicity with two polystyrene backbones, *Angew. Chem. Int. Ed.*, 2000, **39**, 1503–1506.

19 J. M. Tsay, M. Trzoss, L. Shi, X. Kong, M. Selke, M. E. Jung and S. Weiss, Singlet oxygen production by peptide-coated quantum dot-photosensitizer conjugates, *J. Am. Chem. Soc.*, 2007, **129**, 6865–6871.

20 W. Fudickar and T. Linker, Remote substituent effects on the photooxygenation of 9,10-diarylanthracenes: strong evidence for polar intermediates, *Chem. Commun.*, 2008, 1771–1773; B. M. Monroe, Rates of reaction of singlet oxygen with olefins, *J. Phys. Chem.*, 1978, **82**, 15–18.

21 I. E. Kochevar, M. C. Lynch, S. G. Zhuang and C. R. Lambert, Singlet oxygen, but not oxidizing radicals, induces apoptosis in HL-60 cells, *Photochem. Photobiol.*, 2000, **72**, 548–553.

22 G. Hacker, The morphology of apoptosis, *Cell Tissue Res.*, 2000, **301**, 5–17.

23 G. Majno and I. Joris, Apoptosis, oncosis and necrosis. An overview of cell death, *Am. J. Pathol.*, 1995, **146**, 3–15.

24 The reported experimental results were qualitatively reproducible. In order to achieve a quantative assessment of the phototoxicity induced by the new materials, a cell viability assay, such as the MTT assay (9b), should be used.

